Conference Record

Twenty-fourth Asilomar Conference on Signals, Systems & Computers

NOVEMBER 5 - 7, 1990

PACIFIC GROVE, CALIFORNIA

Volume 1 of 2

IEEE Computer Society Order Number 2180
Library of Congress Number 90-0112987
IEEE Catalog Number 90-CH2988-4
ISBN 0-8186-2180-4

THE COMPUTER SOCIETY OF THE IEEE

THE INSTITUTE OF ELECTRICAL AND ELECTRONICS ENGINEERING, INC.

MAPLE PRESS

Performance of Optimum and Adaptive Frequency-Shift Filters for Cochannel Interference and Fading

W. A. Gardner and S. Venkataraman

Department of Electrical Engineering and Computer Science
University of California, Davis
Davis, CA 95616

ABSTRACT

Analog and digital carrier modulated signals, such as AM, digital QAM, PSK, and FSK, exhibit correlation among spectral components separated by multiples of the keying rate and separated by the doubled carrier frequency plus multiples of the keying rate. This spectral redundancy can be exploited to facilitate rejection of cochannel interference, while maintaining minimal signal distortion. It also can be exploited to mitigate the effects of frequency-selective fading with minimal noise amplification. The spectral redundancy is exploited by filtering and adding frequency-shifted versions of the corrupted data. This paper presents the results of a study to evaluate the performance capabilities of optimum and adaptive frequency-shift filters for severely corrupted carrier-modulated signals including AM, BPSK, and QPSK.

I. INTRODUCTION

Modulated signals encountered in most communication and telemetry systems are appropriately modeled as cyclostationary random signals, and as such are inherently spectrally redundant. That is, spectral components in some bands are highly correlated with those in other bands. This spectral redundancy can be exploited by employing frequency-shifting operations, as well as the usual frequency-weighting and phase-shifting operations performed by conventional filters, to obtain substantial reductions in interference with minimal signal distortion. It can be shown theoretically that pairs of some signals, such as AM, ASK, PSK, and digital QAM can in many cases be perfectly separated from each other in spite of severe spectral overlap (exceeding 50%). The theory of spectral correlation and optimum frequency-shift filtering is presented in [1] and [2], and it is explained in [2] how some receiving systems currently in use in digital communication systems, namely the matched-filter/periodic-sampler/sampled-data-filter and the fractionally-spaced equalizer, inherently exploit spectral redundancy, although this is often not recognized.

In this paper, we present the results of a study to evaluate the performance capabilities of optimum and adaptive frequency-shift filters for digital communication. In Section II, the design equation and performance formula for optimum frequency-shift filtering are briefly reviewed. Then in Section III, the results of numerically solving the design equation and substituting the solution into the performance formula to numerically evaluate the minimum-mean-squared-error performance for separation of cochannel BPSK, QPSK, and AM signals are presented. The results cover a wide variety of operating conditions including small and large excess bandwidths of the BPSK and QPSK signals and interferences, equal and unequal carrier frequencies and baud rates of the signals and interferences, differing amounts of spectral overlap (ranging from 50 percent to 100 percent) between the signals and the interferences, and various numbers of frequency shifts used in the receiving filter. These results demonstrate the ability of frequency-shift filtering to obtain excellent performance from an otherwise inoperative system.

In Section IV, two specific scenarios of cochannel interference, namely strong independent partial-band interference and self-interference from multipath propagation resulting in a deep partial-band fade, are considered. The mean-squared-errors and bit-error rates after convergence of LMS-adaptive frequency-shift filters of various lengths, which are implemented as fractionally-spaced equalizers, and LMS-adaptive baud-spaced equalizers are presented. These results demonstrate that the frequency-shift filter can obtain substantial improvements in performance relative to the baud-spaced equalizer which cannot exploit spectral redundancy.

II. OPTIMUM FRESH FILTERING

It is well known that optimum filters for stationary signals are time-invariant. Similarly, optimum filters for signals that exhibit cyclostationarity with a single period (or multiple incommensurate periods) are singly (multiply) periodically time-variant [1] - [4]. A multiply-periodic time-variant (MPTV) linear filter, with input-output relation

$$y(t) = \int_{-\infty}^{\infty} h(t, u)x(u)du \ , \tag{1}$$

has impulse-response function h(t,u) that can be expanded in a Fourier series

$$h(t, u) = \sum_{\eta} h_{\eta}(t-u) \exp(i2\pi\eta u) \ ,$$

$$h_{\eta}(\tau) = \langle h(t+\tau, t) \exp(-i2\pi\eta t) \rangle \ , \tag{2}$$

where $\langle\cdot\rangle$ denotes average over all t, and where the sum ranges over all integer multiples of each fundamental frequency 1/T corresponding to each period T. Substituting (2) into (1) yields the general input-output relation for MPTV linear filters:

$$y(t) = \sum_{\eta} \int_{-\infty}^{\infty} h_{\eta}(t-u) [x(u) \exp(i2\pi\eta u)] du \ .$$

$$= \sum_{\eta} h_{\eta}(t) \otimes x_{\eta}(t) \ , \tag{3a}$$

24ACSSC-12/90/0242 $1.00

where $\otimes$ denotes convolution and $x_\eta(t) \triangleq x(t)\exp(i2\pi\eta t)$ is a frequency-shifted version of x(t). Considering for the moment finite-energy signals, which are Fourier transformable, we can equate the Fourier transforms of both sides of (3a) to obtain

$$Y(f) = \sum_\eta H_\eta(f)\, X(f-\eta) \ . \qquad (3b)$$

Thus, the input is subjected to a number of frequency-shifting (by amount η) operations, each followed by a linear time-invariant filtering operation (with impulse-response function $h_\eta(\cdot)$ and transfer function $H_\eta(\cdot)$), and the results are added together. Consequently, MPTV filtering is equivalent to the FREquency-SHift (FRESH) filtering discussed in Section I. From this, we see that the periodic time variations in an optimum filter for a signal that exhibits cyclostationarity provide the means (viz., frequency shifting) by which the spectral redundancy of such signals can be exploited.

It is well known that linear time-invariant filtering of a real signal is equivalent to linear time-invariant filtering of its analytic signal which in turn is equivalent to linear time-invariant filtering of its complex envelope. But, this is not true for time-variant filtering. In general, linear time-variant filtering of a real signal is equivalent to distinct linear time-variant filtering of each of the complex envelope (or analytic signal) and its complex conjugate. Consequently, if complex signals are to be used, then the problems of optimum and adaptive time-variant (MPTV) filtering must be approached as bivariate filtering problems, where a signal and its conjugate are jointly filtered to produce another signal (and its conjugate) [5]. This is referred to as linear-conjugate-linear (LCL) filtering [6], [7].

The general form for the LCL-MPTV filtering of a complex signal x(t) to produce an estimate $\hat{d}(t)$ of some desired signal d(t) is then (cf. (3a))

$$\hat{d}(t) = \sum_{m=1}^{M} a_m(t) \otimes x_{\alpha_m}(t) + \sum_{n=1}^{N} b_n(t) \otimes x^*_{-\beta_n}(t) \ , \qquad (4)$$

where $(\cdot)^*$ denotes complex conjugation, and where M and N can be infinite. The filter is completely specified by the numbers M and N, the values $\{\alpha_m\}$ and $\{\beta_m\}$ of the periodicity frequencies (or frequency-shift parameters), and the impulse-response functions $\{a_m(t)\}$ and $\{b_n(t)\}$, or their Fourier transforms—the transfer functions—$\{A_m(f)\}$ and $\{B_n(f)\}$.

For specified M, N, $\{\alpha_m\}$, and $\{\beta_n\}$, the optimum LCL-MPTV filtering problem is equivalent to the multivariate (dimension = M + N) Wiener filtering problem [1].

Using the vector concatenations,

$$\underset{\sim}{h}(t) = [\, a_1(t), \ \dots \ , a_M(t), \ b_1(t), \ \dots \ , b_N(t)\,]'$$

$$\underset{\sim}{z}(t) = [\, x_{\alpha_1}(t), \ \dots \ , x_{\alpha_M}(t), \ x^*_{-\beta_1}(t), \ \dots \ , x^*_{-\beta_N}(t)\,]' \ ,$$

where $[\cdot]'$ denotes matrix transposition, (4) can be reexpressed as $\hat{d}(t) = \underset{\sim}{h}'(t) \otimes \underset{\sim}{z}(t)$, and the vector of transfer functions that minimizes the time-averaged squared error between $\hat{d}(t)$ and d(t) is given by the solution to the N + M simultaneous linear equations

$$\underset{\sim}{S}'_{zz}(f)\ \underset{\sim}{H}(f) = \underset{\sim}{S}_{dz}(f) \ , \qquad (5)$$

where $\underset{\sim}{S}_{zz}(f)$ and $\underset{\sim}{S}_{dz}(f)$ are the auto- and cross-spectral density matrices obtained by Fourier transforming the correlations

$$\underset{\sim}{R}_{zz}(\tau) \triangleq \langle\, \underset{\sim}{z}(t+\tau/2)\ \underset{\sim}{z}^\dagger(t-\tau/2)\,\rangle$$

$$\underset{\sim}{R}_{dz}(\tau) \triangleq \langle\, d(t+\tau/2)\ \underset{\sim}{z}^*(t-\tau/2)\,\rangle \ ,$$

where $(\cdot)^\dagger$ denotes matrix transposition and conjugation. Substituting the definition of z(t) in terms of x(t) into (5) yields the equivalent optimum LCL-MPTV filtering equations:

$$\sum_{m=1}^{M} S_x^{\alpha_k-\alpha_m}\left(f - \frac{\alpha_m+\alpha_k}{2}\right) A_m(f) + \sum_{n=1}^{N} S_{xx^*}^{\beta_n-\alpha_k}\left(f - \frac{\beta_n+\alpha_k}{2}\right)^* B_n(f) = S_{dx}^{\alpha_k}\left(f-\frac{\alpha_k}{2}\right), \qquad k = 1, 2, \dots, M, \quad (6a)$$

$$\sum_{m=1}^{M} S_{xx^*}^{\beta_k-\alpha_m}\left(f - \frac{\alpha_m+\beta_k}{2}\right) A_m(f) + \sum_{n=1}^{N} S_x^{\beta_k-\beta_n}\left(-f + \frac{\beta_n+\beta_k}{2}\right) B_n(f) = S_{dx^*}^{\beta_k}\left(f-\frac{\beta_k}{2}\right), \qquad k = 1, 2, \dots, N \ , \quad (6b)$$

which are fully specified in terms of the spectral correlation density functions for x(t) and d(t), which are defined by

$$S_{xy}^{\alpha}(f) \stackrel{\Delta}{=} \lim_{T\to\infty} T \langle\, X_T(t, f+\alpha/2)\, Y_T^*(t, f-\alpha/2)\rangle \qquad (7)$$

$$= \int_{-\infty}^{\infty} R_{xy}^{\alpha}(\tau)\exp(-i2\pi f\tau)d\tau \ , \qquad (8)$$

where

$$X_T(t, \nu) \triangleq \frac{1}{T}\int_{t-T/2}^{t+T/2} x(u)\exp(-i2\pi\nu u)du \ , \qquad (9)$$

and

$$R_{xy}^{\alpha}(\tau) \triangleq \langle\, x(t+\tau/2)\, y^*(t-\tau/2)\exp(-i2\pi\alpha t)\,\rangle \qquad (10)$$

The spectrum of the error $e(t) \triangleq \hat{d}(t) - d(t)$ whose mean squared value is minimized by the multivariate Wiener filter is [1]

$$S_e(f) = S_d(f) - \underset{\sim}{S}^\dagger_{dz}(f)\underset{\sim}{H}(f) \ ,$$

which can be expressed more explicitly as

$$S_e(f) = S_d(f) - \sum_{m=1}^{M} S_{dx}^{\alpha_m}\left(f - \frac{\alpha_m}{2}\right)^* A_m(f) - \sum_{n=1}^{N} S_{dx^*}^{\beta_n}\left(f - \frac{\beta_n}{2}\right)^* B_n(f) \ . \qquad (11)$$

The problem of selecting the best finite sets of frequency-shift parameters $\{\alpha_m\}$ and $\{\beta_n\}$ is an important one in practice, as illustrated in Section III, but is not easy to characterize mathematically.

It follows from the derivation of the optimum FRESH filtering equations (6), in terms of multivariate Wiener filtering, that adaptive implementations of FRESH filters can easily be obtained from conventional multivariate adaptive filters. Thus, a basic adaptively adjustable structure is simply a parallel bank of N + M frequency-shifting product-modulators each followed by an FIR filter, the outputs of which are summed. The N + M FIR filters can be jointly adapted using standard algorithms such as the LMS, as demonstrated in Section IV.

III. OPTIMUM PERFORMANCE FOR SEPARATION OF COCHANNEL AM, BPSK, AND QPSK

In this section, we present the results of numerically solving the design equation (6) and using the solution to numerically evaluate the performance formula for the MSE which is given by the integral of (11). We consider sums of two or three real AM signals, or two complex BPSK signals, or two complex QPSK signals, in additive white Gaussian noise. We consider one of the two or three spectrally overlapping signals to be the signal of interest (SOI), and we consider the remaining one or two signals to be signals not of interest (SNOI). All signals for each scenario considered have the same power spectral density, which is either triangle-shaped (for AM and BPSK/QPSK with 300% excess bandwidth), or raised-cosine-shaped (for BPSK/QPSK with 25% and 100% excess bandwidth)*, the same excess bandwidth (EBW) of either 25 percent, 100 percent, or 300 percent, and the same SNR of 20 dB. However, the absolute bandwidths, as determined by the baud rates, are the same in some cases and different in others. The same is true of the carrier frequencies.

In Figures 1 – 3, we show the minimum Mean-Squared-Error (MSE) in dB versus the number of frequency shifts used in the complex LCL FRESH filter for the case of one SOI and one SNOI, both of which are either complex BPSK or complex QPSK. The values of the frequency-shifts used are specified in Table I for Figure 1, Table II for Figure 2, and Table III for Figure 3. In these tables, the frequency shift having value 0 corresponds to the linear time-invariant (LTI) path for QPSK and it corresponds to both the LTI and LCLTI paths for BPSK. Similarly, for BPSK, each frequency-shift value listed is used in both the conjugate and nonconjugate paths. There are no conjugate paths for QPSK. Thus, in terms of the number-of-shifts parameter N in Figures 1 – 3, the number of actual filter paths for QPSK is N+1, but for BPSK it is 2(N+1) for all $N > 1$, and it is N+1 for $N \leq 1$. However, since both the phases and frequencies of the carriers are equal in Figure 3, the conjugate path is of no use for BPSK. The order of frequency shifts has been chosen to maximize the rate of decrease of MSE with an increase in N. The carrier frequency and baud rate of the SOI are $f_* = 0$ and $f_1 = 1/(1+e)$, where e = 1/4, 1, 3 for excess bandwidths of 25%, 100%, and 300%, respectively. The two-sided bandwidth of the SOI is unity. In cases where the carrier frequency or baud rate of the SNOI are different from those of the SOI, their values are $f_0 = 0.2257$ and $f_2 = 0.753/(1+e)$, respectively, where 0.753 is the two-sided bandwidth of the SNOI.

The best performance is attainable when the two carrier frequencies are different regardless of whether the baud rates are the same or different. The performance for these two cases is shown in Figures 1 and 2 where it can be seen that very little improvement relative to the LTI filter is available for QPSK with 25% EBW (since there is no spectral redundancy associated with the carriers and little associated with the baud rates because of the low EBW), but substantial improvement (14 dB – 16 dB) is available for QPSK with 100% EBW. For BPSK with 25% EBW, about 17 dB – 18 dB improvement is available, and this increases to about 20 dB for 100% EBW, and about 22 dB -- 23 dB for 300% EBW. Since the SNR is 20 dB, this reveals that the SNOI is essentially eliminated for all EBWs for BPSK, but only for EBW ≥ 100% for QPSK.

The performance is not quite as good when the two carrier frequencies are the same unless the EBW exceeds 100%, but substantial improvement relative to the LTI filter is still attainable for EBWs on the order of 100%. The performance for this case is shown in Figure 3, where it can be seen that there is little improvement relative to the LTI filter for either BPSK or QPSK when the EBW is low (25%). But, when the EBW is increased to 100%, an improvement of 6 dB – 7 dB is available, and this increases to 16 dB – 19 dB for EBW = 300%, in which case the SNOI is very nearly eliminated.

In Figure 4, we show the minimum MSE versus the number of frequency shifts used in a real FRESH filter for one real AM SNOI and three cases of one or two real AM SNOIs. For cases 1 and 2, the first SNOI spectrally overlaps the real AM SOI and the second SNOI overlaps the first SNOI, but not the SOI. The amount of overlap of the SOI and first SNOI is 77 percent and the overlap of the first and second SNOIs is 16 percent for case 1. For case 2, the SOI and first SNOI overlap 20 percent and the first and second SNOIs overlap 65 percent. For case 3, there is only one SNOI and it overlaps the SOI by 77 percent. The bandwidths of all three AM signals are unity, the carrier frequency of the SOI is $f_1 = 0.75$, and the carrier frequencies of the SNOI are denoted by f_2 and f_3. The particular values of frequency shifts used in Figure 4 are shown in Table IV.

As can be seen from Figure 4, excellent performance is attainable when there is only one SNOI, which overlaps the SOI by 77 percent. In this case (case 3) the SNOI is very nearly eliminated with the use of only 3 frequency shifts ($\alpha = 0$ and $\alpha = \pm 2f_1$). However, when two SNOI are present, about 9 frequency shifts are needed to approach the best attainable performances, but the SNOI is essentially eliminated in case 2, whereas it is not suppressed nearly as well for case 1, although the improvement relative to the LTI filter is still 13 dB in case 1. The reason for this is that although the two SNOI in case 1 substantially overlap each other in the frequency domain, the one that overlaps the SOI overlaps it only 20 percent, whereas in case 1 the overlap of the two SNOI is minimal, but the one that overlaps the SOI overlaps it 77 percent. Similar results have been obtained for complex LCL FRESH filtering of complex AM signals. Specifically, with $f_1 = 0$, $f_2 = 0.5$, $f_3 = 0.75$, and unity bandwidths (i.e., 50% overlap between first SNOI and SOI, and 75% overlap between the two SNOI), frequency shifts of $0, \pm 2f_2$ in both linear and conjugate linear filters yields MSE = –21.5 dB. But, with $f_2 = 0.2257$ and $f_3 = 1.0$ (i.e., 77% overlap between first SNOI and SOI, and 23% overlap between the two SNOI), it takes nine frequency shifts (including combinations of both f_2 and f_3) in both linear and conjugate linear filters to obtain MSE = –18.8 dB.

* For BPSK and QPSK, these shapes are the squared magnitudes of the pulse transforms (keying-envelope transforms) since the digital data sequence is white. These particular shapes result in zero intersymbol interference at the output of a matched filter.

IV. ADAPTIVE FILTERING PERFORMANCE FOR COCHANNEL INTERFERENCE AND FADING

In this section, we consider a BPSK SOI with a carrier offset frequency of zero and a raised-cosine-shaped pulse transform with 100% EBW in additive complex Gaussian noise and partial-band interference, or fading, and a complex FRESH filter that exploits the spectral correlation among only those spectral components that are separated by integer multiples of the baud rate of the SOI. Since this corresponds to all the exploitable spectral correlation in QPSK and other digital QAM signals, and since the spectral correlation characteristics of all these signals are identical when their pulse shapes (keying envelopes) are identical, then the results reported here for BPSK can be qualitatively extrapolated to these other signals.

Since the ultimate goal in combatting cochannel interference and fading for digital data signals is to reliably extract the digital data sequence, only this sequence rather than the entire waveform needs to be estimated. This means that the FRESH filter will be followed by a baud-rate sampler. This fact coupled with the preceding decision to use only frequency shifts that are harmonics of the baud rate results in a simplification of the FRESH filter, as explained next.

Because no spectral correlation associated with the carrier is to be exploited, linear filtering rather than LCL filtering is adequate. Furthermore, since the absolute bandwidth of the BPSK signal is finite, both the bandwidth and number of frequency shifts in the linear FRESH filter are finite. In this case, it is shown in [2] that the FRESH filter followed by a baud-rate sampler is exactly equivalent to what is called a Fractionally-Spaced Equalizer (FSE), cf. [8]. Since the EBW of the BPSK signal is 100 percent, the sampling rate at the input to the FSE is twice that at the output, and the output rate equals the baud rate f_1. This is equivalent to a FRESH filter with frequency shifts of 0, $\pm f_1$, followed by a baud-rate sampler.

Because of this equivalence, the FSE structure was used for simulating the adaptive FRESH filter in this study. In order to illustrate the degree of improvement in performance obtainable by exploiting spectral correlation, a conventional adaptive baud-spaced equalizer (BSE) was also simulated in this study. The BSE is preceded by an antialiasing filter and a baud-rate sampler.

The filter memory length in units of baud intervals is denoted by N. This means that the FSE has 2N adaptive weights, whereas the BSE has N adaptive weights. The LMS algorithm for adaptation of these weights was used. An ideal replica of the digital data sequence was used as the training data in order to remove the effects of imperfect training data on the performance.

The LMS algorithm was iterated for 2,048 bauds and the MSE (between the symbol sequence and the baud-rate samples) and bit-error-rate (BER) were computed over the subsequent 6,144 bauds.

In the first case considered, the partial-band interference is an AM signal with center frequency $f_0 = 0.1247f_1$ and bandwidths $\Delta = f_1/4$ and $f_1/8$, where f_1 is the baud rate of the BPSK SOI. The SNR is 20 dB and the Signal-to-Interference Ratio (SIR) is 0 dB. The results obtained are shown in Table V, where it can be seen that the FSE outperforms the BSE by a substantial margin.

In the second case considered, we have self interference caused from multipath propagation and resulting in an infinitely deep fade throughout the same band where the AM interference was present in the first case. The SNR is again 20 dB. Essentially, the same performance as in the first case was obtained.

V. CONCLUSIONS

It has been shown by both thorough numerical performance evaluation of optimized frequency-shift filters and by limited simulations of adaptive frequency-shift filters that severe cochannel interference can be removed from a signal without introducing substantial distortion, and that severe frequency-selective fading can be mitigated without substantial noise amplification. The signal corruption that is so effectively removed by frequency-shift filters, which exploit spectral redundancy, can render inoperable systems that use only conventional filters, which cannot exploit spectral redundancy.

More specifically, it has been shown that effective separation of two BPSK or QPSK signals is possible regardless of the relationships between their carrier frequencies and baud rates provided that for QPSK the excess bandwidths are at least 100% [although if both their carrier frequencies and baud rates are identical—a case not considered in this paper—and their pulse shapes or keying envelopes are also identical, then either their carrier phases (for BPSK) or their keying phases must be distinct]. It is also easily proved that L individual PSK or digital QAM signals with equal baud rates, but arbitrary carrier frequencies, can be separated if their excess bandwidth is at least (L–1)100%. The proof follows immediately from the fact that by considering infinitesimal bands separated by integer multiples of the baud rate, we can obtain L linear equations in L unknowns, since the infinitesimally narrowband components from each signal in the L infinitesimal bands are perfectly correlated (cf. [1]) and are, therefore, just scaled versions of each other. (If the carrier frequencies are equal, then it is required that the L signal pulses be distinct; e.g., they could have distinct timing offsets.)

REFERENCES

[1] W. A. Gardner, *Statistical Spectral Analysis: A Nonprobabilistic Theory*, Englewood Cliffs, N.J.: Prentice-Hall, 1987.

[2] W. A. Gardner and W. A. Brown, "Frequency-shift filtering theory for adaptive cochannel interference removal," *Proceedings of Twenty-Third Asilomar Conference on Signals, Systems, and Computers*, Oct. 30 – Nov. 1, 1989, Pacific Grove, CA, pp.562-567.

[3] W. A. Gardner, *Introduction to Random Processes with Applications to Signals and Systems*, second ed., New York: McGraw-Hill, 1989.

[4] W. A. Gardner and L. E. Franks, "Characterization of cyclostationary random signal processes," *IEEE Transactions on Information Theory*, Vol. IT-21, pp. 4-14, 1975.

[5] W. A. Brown, "On the theory of cyclostationary signals," Ph.D. Dissertation, 1987, Department of Electrical Engineering and Computer Science, University of California, Davis.

[6] W. M. Brown, "Conjugate linear filtering," *IEEE Transactions on Information Theory*, Vol. IT-15, pp. 462-465, 1969.

[7] W. M. Brown, *Analysis of Linear Time-Variant Systems*, New York: McGraw-Hill, 1963.

[8] R. D. Gitlin and S. B. Weinstein, "Fractionally-spaced equalization: An improved digital transversal equalizer," *The Bell System Technical Journal*, Vol. 60, pp. 275-296, 1981.

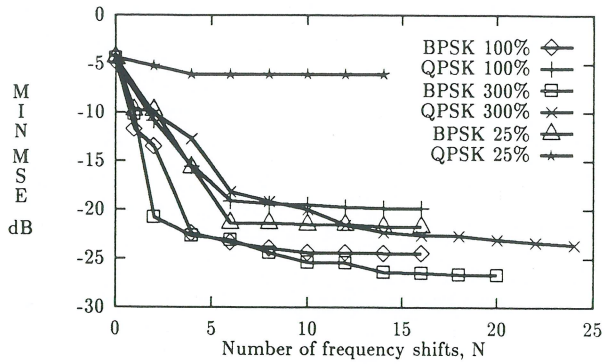

Figure 1: Minimum MSEs for complex BPSK and QPSK signals with EBWs of 25%, 100%, and 300%, versus the number of frequency shifts used. The SOI and SNOI have different baud rates and different carrier frequencies. SNOI overlaps the SOI 60%

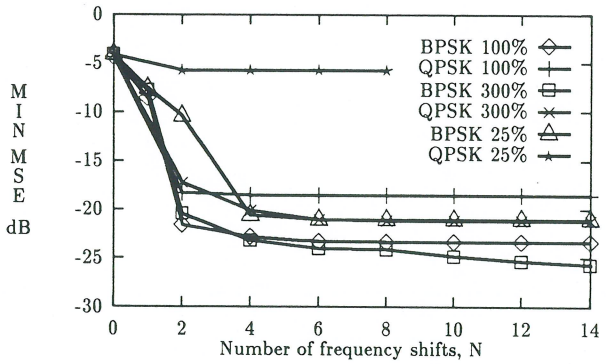

Figure 2: Same as Figure 1 except the baud rates are equal. SNOI overlaps the SOI 87%

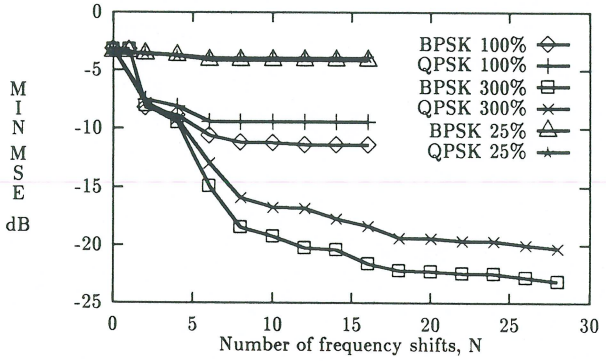

Figure 3: Same as Figure 1 except the carrier frequencies are equal. SNOI overlaps the SOI 75%

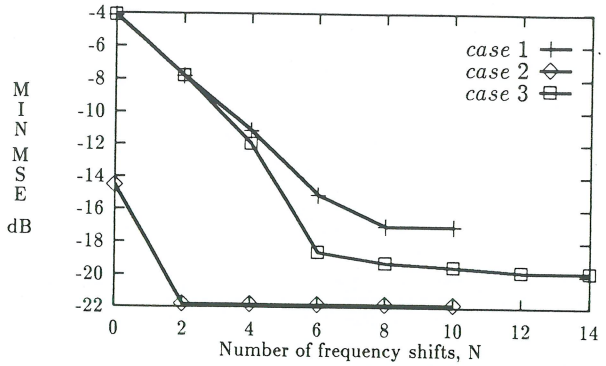

Figure 4: Minimum MSE for real AM SOI and AM SNOIs versus the number of frequency shifts used. Case 1: $f_2 = 0.975, f_3 = 1.81$. Case 2: $f_2 = 1.55, f_3 = 1.9$. Case 3: $f_2 = 0.975$.

Table I: Frequency-shift values in the order they appear in Figure 1. Frequencies f_1 and f_2 are the baud rates and 0 and f_0 are the carrier frequencies of the SOI and SNOI, respectively.

QPSK 25%:	$0, \pm f_1, \pm f_2, \pm(f_1-f_2), \pm(f_1+f_2), \pm(2f_1-f_2), \pm(f_1-2f_2), \pm(2f_1-2f_2)$
BPSK 25%:	$0, \pm f_1, \pm f_2, \pm 2f_0, \pm(2f_0+f_2), \pm(2f_0-f_2), \pm(2f_0+f_1), \pm(2f_0-f_1), \pm(f_1-f_2)$
QPSK 100%:	$0, \pm f_1, \pm f_2, \pm(f_1-f_2), \pm(f_1+f_2), \pm(2f_1-f_2), \pm(f_1-2f_2), \pm 2(f_1-f_2), \pm 2(f_1+f_2)$
BPSK 100%:	$0, \pm f_1, \pm f_2, \pm(f_1-f_2), \pm 2f_0, \pm(2f_0-f_1), \pm(2f_0+f_1), \pm(2f_0-f_2), \pm(2f_0+f_2)$
QPSK 300%:	$0, \pm f_1, \pm f_2, \pm 2f_1, \pm(f_1-f_2), \pm(f_1+f_2), \pm(2f_1-f_2), \pm(f_1-2f_2), \pm 2(f_1-f_2), \pm 2(f_1+f_2), \pm(3f_1-2f_2), \pm(2f_1-3f_2), \pm 3f_1$
BPSK 300%:	$0, \pm f_1, \pm f_2, \pm 2f_0, \pm(2f_0+f_1), \pm(2f_0-f_1), \pm(2f_1-f_2), \pm 2f_1, \pm 2f_2, \pm 3f_1, \pm 3f_2$

Table II: Frequency-shift values in the order they appear in Figure 2. Frequency f_1 is the baud rate for both SOI and SNOI, and 0 and f_0 are the carrier frequencies of the SOI and SNOI, respectively.

QPSK 25%:	$0, \pm f_1, \pm 2f_1, \pm 3f_1, \pm 4f_1$
BPSK 25%:	$0, \pm f_1, \pm 2f_0, \pm(2f_0-f_1), \pm(2f_0+f_1), \pm 2f_1, \pm 3f_1$
QPSK 100%:	$0, \pm f_1, \pm 2f_1, \pm 3f_1, \pm 4f_1, \pm 2f_0, \pm(2f_0-f_1), \pm(2f_0+f_1)$
BPSK 100%:	$0, \pm f_1, \pm 2f_0, \pm(2f_0-f_1), \pm(2f_0+f_1), \pm 2f_1, \pm 3f_1, \pm 4f_1$
QPSK 300%:	$0, \pm f_1, \pm 2f_1, \pm 3f_1, \pm 4f_1, \pm 2f_0, \pm(2f_0-f_1), \pm(2f_0+f_1)$
BPSK 300%:	$0, \pm f_1, \pm 2f_1, \pm 3f_1, \pm 4f_1, \pm 2f_0, \pm(2f_0-f_1), \pm(2f_0+f_1)$

Table III: Frequency-shift values in the order they appear in Figure 3. Frequencies f_1 and f_2 are the baud rates of the SOI and SNOI, respectively, and the carrier frequencies of both the SOI and SNOI are zero.

QPSK 25%:	$0, \pm f_1, \pm f_2, \pm(f_1-f_2), \pm(2f_1-f_2), \pm(f_1-2f_2), \pm 2(f_1-f_2), \pm(f_1+f_2), \pm 2(f_1+f_2)$
BPSK 25%:	$0, \pm f_1, \pm f_2, \pm(f_1-f_2), \pm(2f_1-f_2), \pm(f_1-2f_2), \pm 2(f_1-f_2), \pm(f_1+f_2), \pm 2(f_1+f_2)$
QPSK 100%:	$0, \pm f_1, \pm f_2, \pm(f_1-f_2), \pm(2f_1-f_2), \pm(f_1-2f_2), \pm 2(f_1-f_2), \pm(f_1+f_2), \pm 2(f_1+f_2)$
BPSK 100%:	$0, \pm f_1, \pm f_2, \pm(f_1-f_2), \pm(2f_1-f_2), \pm(f_1-2f_2), \pm 2(f_1-f_2), \pm(f_1+f_2), \pm 2(f_1+f_2)$
QPSK 300%:	$0, \pm f_1, \pm f_2, \pm(f_1-f_2), \pm(f_1+f_2), \pm 2f_1, \pm(2f_1-f_2), \pm(f_1-2f_2), \pm 2(f_1-f_2), \pm 2(f_1+f_2), \pm(3f_1-2f_2), \pm(2f_1-3f_2), \pm 3f_1, \pm 3f_2, \pm 2f_2$
BPSK 300%:	$0, \pm f_1, \pm f_2, \pm(f_1-f_2), \pm(f_1+f_2), \pm 2f_1, \pm(2f_1-f_2), \pm(f_1-2f_2), \pm 2(f_1-f_2), \pm 2(f_1+f_2), \pm(3f_1-2f_2), \pm(2f_1-3f_2), \pm 3f_1, \pm 3f_2, \pm 2f_2$

Table IV: Frequency-shift values in the order they appear in Figure 4. Frequency f_1 is the carrier frequency of the SOI and f_2 and f_3 are the carrier frequencies of the two SNOI.

Two SNOI, Cases 1, 2:	$0, \pm 2f_1, \pm 2f_2, \pm 2(f_2-f_1), \pm 2(f_2-f_3), \pm 2(f_1-f_3)$
One SNOI, Case 3:	$0, \pm 2f_1, \pm 2f_2, \pm 2(f_2-f_1), \pm 2(f_2-2f_1), \pm 2(2f_2-f_1), \pm 4(f_2-f_1), \pm 2(2f_2-3f_1)$

Table V: MSE and BER after convergence of LMS algorithm for BPSK signal plus AM interference (SIR = 0 dB) and noise (SNR = 20 dB). Δ = AM bandwidth, f_1 = BPSK baud rate, N = filter length in bauds. * indicates no bit error in 6,144 bits (BER < 1.6×10^{-4}). The value in parenthesis is the minimum attainable MSE (for N = ∞).

Δ			N=4	8	12	16	20
$\frac{f_1}{4}$	F	BER	*	*	*	*	*
	S	MSE	−9.8	−11	−11	−11	−11
	E	(−11)					
	B	BER		2.4×10^{-2}	6.3×10^{-3}	2.3×10^{-3}	1.3×10^{-3}
	S	MSE		−4.6	−5.4	−6.1	−6.3
	E	(−6.3)					
$\frac{f_1}{8}$	F	BER	*	*	*	*	*
	S	MSE	−11	−13	−13	−13	−13
	E	(−14)					
	B	BER		1.7×10^{-2}	1.8×10^{-3}	6.5×10^{-4}	3.3×10^{-4}
	S	MSE		−5.2	−7.4	−8.0	−8.2
	E	(−8.9)					